

Experimental Study on the Heat Transfer Enhancement in Sub-Channels of 6×6 Rod Bundle with Large Scale Vortex Flow Mixing Vanes

Sun-Joon Byun^{a*}, Jung Yoon^a, Hyungmo Kim^a and Ji-Young Jeong^a

^aKorea Atomic Energy Research Institute, 989-11 Daedeok-daero, Yuseong-gu, Daejeon, 305-353

*Corresponding author: sjbyun81@kaeri.re.kr

1. Introduction

The Pressurized Water Reactor (PWR) fuel assembly consists of fuel rods, control rods, and spacer grids with mixing vanes, as shown in Fig. 1.

The spacer grid in the fuel rod assembly functions in several basic ways: it secures the coolant flow channel, maintains the structural form of the fuel rods, withstands external shocks, and inhibits flow-induced vibrations. The spacer grid also serves to improve the capability to prevent the critical heat flux (CHF).

The occurrence of the critical heat flux in the nuclear reactor could damage the fuel rods by raising the surface temperature of the fuel rod materials to the melting point. Therefore, the thermal margin in the critical heat flux must be sufficient under normal driving conditions so that the occurrence of the critical heat flux is suppressed. For this, a mixing vane is attached to the end of the spacer grid. The mixing vane increases the convective heat transfer by causing a swirling flow and cross flow, which force the current between the reactor sub-channels to mix the coolant, and by promoting the turbulence production. If the geometric shape of the fuel rod bundle and the heat release rate are in the same condition, the overall heat transfer performance of the fuel rods will be governed by the secondary flow induced by the spacer grid [1,2].

In this study, to address these shortcomings of the split mixing vane, using the LSVF mixing vane, a newly introduced mixing vane type, the heat transfer coefficient enhancement of the fuel rod was measured by creating a secondary large scale vortex flow.

This was then compared with the change in local heat transfer coefficient when using the existing mixing vanes. Further, to measure the changes in the heat transfer coefficient by the two mixing vanes, local heat transfer coefficients were calculated by measuring the

coolant temperature and the surface temperature of the fuel rod using copper sensors.

2. Experimental Apparatus and Method

2.1 Experimental Apparatus

The experimental apparatus used in this study consists of an LDV system, reservoir, chiller, pump flow control valve, settling chamber, flow meter, and circulation loop, as shown in Fig 2. As shown in Fig. 3, by the first spacer grid installed at the location $30 D_h$ from the inlet, and the second spacer grid installed at the location $40 D_h$ from the first spacer grid, the flow passes through the sub-channels of the fuel rods with a constant pitch of 21.8 mm. To change the location of the heated copper sensor, the rod length should be changed.

The test section has square duct shape of 140 mm × 140 mm × 1,700 mm. At the test section, a 6 × 6 rod bundle was supported by a spacer grid. The rod diameter is 15.88 mm, which is made larger than that of the actual rod. In addition, for the convenience of the rod replacement, the front surface of the test section was made of transparent acrylic. When replacing a rod, through the transparent acrylic, observation and replacement are possible in the system. The geometry parameters of the test section are shown in Table 1.

The purified water circulates through a 15 HP pump in the experimental apparatus. The water flows in the reservoir were maintained at 24.0 ± 0.2 °C using a chiller.

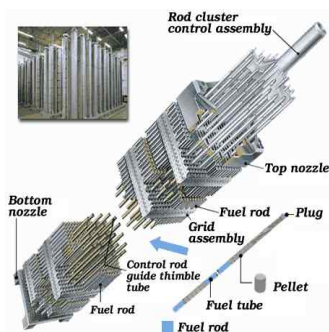
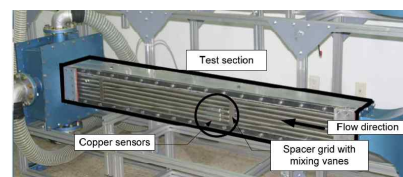
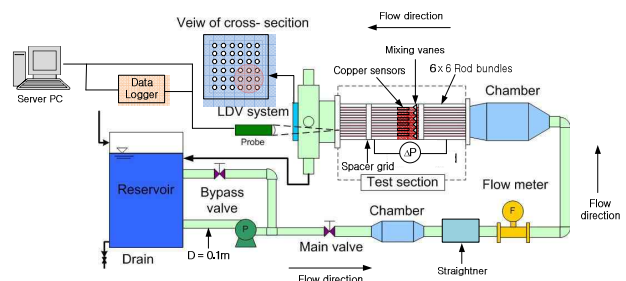


Fig. 1. Typical fuel rod assembly of pressurized light water nuclear reactor



(a) Photograph of test-section



(b) Schematic diagram of experimental apparatus
Fig. 2. Test section and experimental apparatus

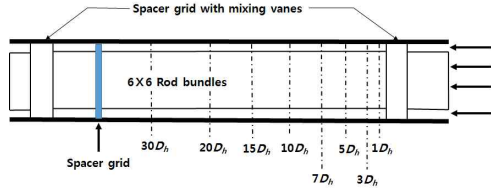


Fig. 3. Locations of measuring points

Table I: Geometry Parameters for the Fuel Rod Bundle

Parameters	Symbol	Unit	Dimension
Rod Diameter	D	mm	15.88
Rod Pitch	P	mm	21.86
Spacer Grid Pitch	P_s	mm	605.1
Housing Height	H	mm	140.0
Hydraulic Diameter	D_h	mm	20.17
Vane Bending Angle	θ	Degree	30.0
Pitch to Diameter	P/d	-	1.38

The flux passing through the test section is adjusted at Reynolds numbers of 30,000 and 50,000 using a flux control valve and a turbine flow meter (TRIMEE Model: TP100S4C121R2).

2.2 Measuring Principle of Local Heat Transfer Coefficient

In this study, an experiment for measuring the local heat transfer coefficient of the fuel rods was conducted under the condition of a constant heat flux. Newton's law of cooling, explaining the heat transfer of fuel rods, is the same as the following Eq. (1):

$$q = hA(T_s - T_m) \quad (1)$$

where h = convective heat transfer coefficient, A = surface area, T_s = surface temperature of the fuel rod, and T_m = the average bulk temperature of the coolant. However, since the surface area and heat flux of the heated copper sensor are consistent, the equation of the heat transfer coefficient can be described as Eq. (2).

$$h = \frac{q}{A(T_s - T_m)} = \frac{C}{(T_s - T_m)} \quad (2)$$

where C is a constant. Meanwhile, the Nusselt number is defined as Eq. (3).

$$Nu = \frac{hD_h}{k} \quad (3)$$

In this formula, k is the heat transfer coefficient of the coolant, and the heat transfer enhancement by the

mixing vane is measured by Nu/Nu_D , the proportion of the Nusselt number which is non-dimensionalized by Nu_D , a Nusselt number in a fully developed flow. The ratio of the Nusselt number is calculated by measuring the temperature, as shown in Eq. (4).

$$\frac{Nu}{Nu_D} = \frac{\frac{hD_h}{k}}{\frac{h_D D_h}{k}} = \frac{h}{h_D} = \frac{T_{sD} - T_{mD}}{T_s - T_m} \quad (4)$$

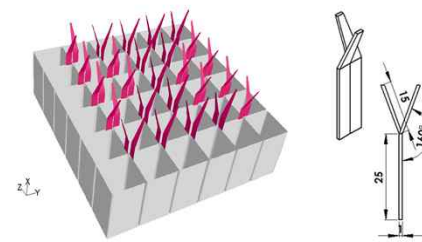
Therefore, Nu/Nu_D , the ratio of the Nusselt number used for the measurement in this study, is determined by the values of T_{sD} , the surface temperature of a heated copper sensor; T_{mD} , the bulk average temperature in fully developed flow; T_s , the surface temperature of a heated copper sensor; and T_m , the bulk mean temperature at each location.

2.3 Measuring of Local Heat Transfer Coefficient

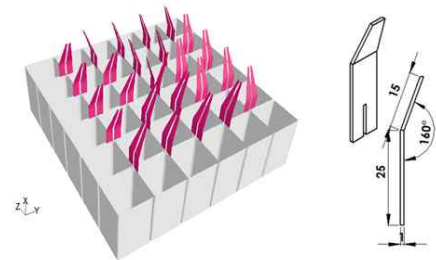
To measure the local heat transfer coefficient, as shown in Fig. 4, a second spacer grid with mixing vanes was installed at the location $40 D_h$ from the first spacer grid with the previous Split mixing vanes and LSVF mixing vanes. Fuel rods were arranged in a square shape with a consistent pitch of 21.80 mm between the rod centers. An interval of 605.1 mm occurs between the two spacer grids.

Local heat transfer coefficient to be measured in a copper sensor was briefly calculated in terms of heat flux and surface temperature as shown in Eq. (5).

$$h(z) = q(z) / A_s [T_s(z) - T_b] \quad (5)$$



(a) Split mixing vanes



(b) LSVF mixing vanes

Fig. 4. Arrangement of Split mixing vanes and LSVF mixing vanes

$$Nu(z) = \frac{h(z)D_h}{k(z)} \quad (6)$$

$$Nu(z) = \frac{q}{A_s(T_s - T_m)} \frac{D_h}{k} = \frac{qD_h}{A_s k} \frac{1}{\theta} = \frac{C}{\theta(z)} \quad (7)$$

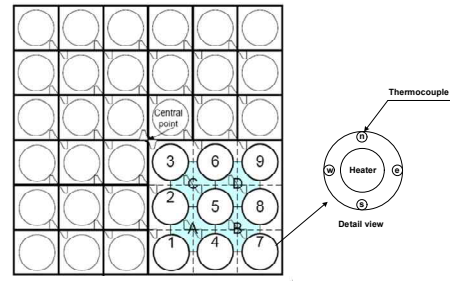
T_b is defined as bulk temperature of the axial location of $z/D_h = 40$ from the downstream of a spacer grid using the unheated copper sensor. It means that measured temperature in fully developed condition was equal to all test case of same heat flux condition. In order to measure local heat transfer coefficients in rod bundles with mixing vanes, local Nusselt number was defined as Eq. (6). Eq. (6) shows Nusselt number with the characteristics length scale of a hydraulic diameter. $h(z)$ is represented as function of convective heat transfer coefficient for an axial location of z . $q(z)$ means total heating rate.

$Nu(z)$ is presented as a simple function of the difference temperature between the surface temperature and the bulk temperature such like Eq. (7). If the surface temperature were measured, local Nusselt number is able to be measured.

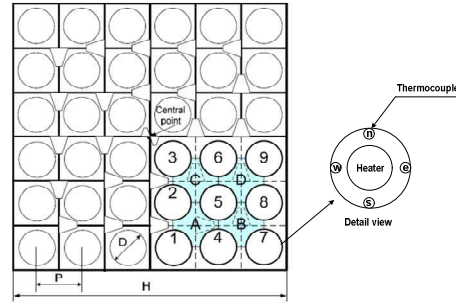
Using copper sensors installed in nine fuel rods, as shown in Fig. 5, the surface temperatures are measured.

The diameter of the copper sensors used in this study is 15.88 mm, and their total length is 70.0 mm. Of the total length of the copper sensor, both sides of the 15.0 mm are connecting parts. For the remaining 40.0 mm, a cartridge heater used as the heat source is located directly at the center to act as the heat source of the heat flux. In addition, to measure the surface temperature of the copper sensor, a T-type thermocouple needs to be installed at a 90° interval directly in the center of the copper sensor in the circumference direction.

In addition, to place a cartridge heater directly in the center of the copper rod, the thermocouple of the cartridge heater was wrapped with asbestos tape. The gap between the copper and the cartridge heater was sealed with thermal grease. The conduction of the heat from the cartridge heater to the surface of the copper sensor was therefore enhanced. Changing the length of both sides of the stainless steel rod connected to the copper sensor enables the location of the copper sensor to be changed. With this principle, every time the copper sensor location is changed, it is possible to conduct a test without disassembling the experimental apparatus; also, as the test is uninterrupted by the flow, it is possible to measure the temperature of the copper sensor surface. To apply a constant heat flux to the copper rod surface by a cartridge, each of the nine heaters to be used in this study needs to be controlled since, even if the cartridge heater is accurately made, the resistance varies slightly. Therefore, to apply a constant heat flux to the copper surface, a constant heat flux could be transferred to the copper sensor surface by controlling the voltage according to the resistance



(a) Arrangement of Split mixing vane



(b) Arrangement of LSVF mixing vane

Fig. 5. Arrangement of mixing vanes for experiment

through the power supply device. The voltage was thus measured through the digital multi-meter (Fluke Model : 2645, error : $\pm 1.0\%$). In this study, Eq. (8) was used to calculate the heat transfer coefficient.

$$h = q / (A_s - T_m) \quad (8)$$

To measure T_m , a copper sensor without a cartridge heater was used. To ensure ΔT , the temperature gap between T_s and T_m was sufficient, 120 W (heat flux 59,864 W/m²) of heat was applied to the cartridge.

3. Experimental Results

To determine the increase in heat transfer performance by a swirling turbulence flow resulting from the generated vortex (by attaching the mixing vanes to a spacer grid to mix and control the flowing direction of the coolant), the characteristics of the heat transfer enhancement were measured when using a spacer grid with the existing Split mixing vanes, and when using a spacer grid with the LSVF mixing vanes.

For locations 1, 3, 5, 7, 10, 15, 20, and 35 D_h from the downstream of a spacer grid, by measuring the temperature of the rod surface at each point and the cooling water temperature in the fully developed flow, the local average Nusselt number was calculated. Fig. 6 show the decay in the average Nusselt number by the Split mixing vane and LSVF mixing vane, respectively, at Reynolds numbers of 30,000. The measured local average Nusselt number was non-dimensionalized by the Nusselt number measured at the location $D_h = 40$ from the downstream of a spacer grid. A comparison of

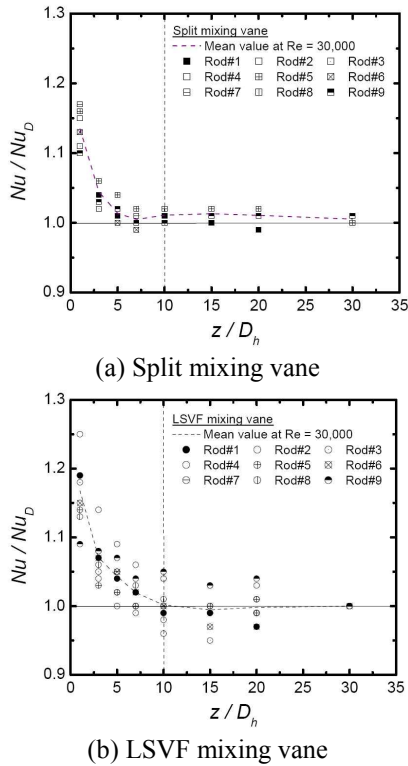


Fig. 6. Axial decay of normalized Nusselt numbers of rod bundles after the spacer grid with Split and LSVF mixing vanes for Reynolds numbers of 30,000

the decay in the dimensionless local average Nusselt number in the sub-channel of the rod bundle with LSVF mixing vanes. As the Reynolds number increases, the heat transfer enhancement of the LSVF mixing vane also further increases.

Fig. 7 shows that the average Nusselt number change is larger in the sub-channel with LSVF mixing vanes than in the Split mixing vanes according to the rod position. In particular, at a Reynolds number of 30,000, the average Nusselt number according to the rod position is larger. This is because the vortex flow intensity differs since a vortex flow with a large length scale by the LSVF mixing vane does not occur evenly in the entire fuel rod sub-channel surface. For a Reynolds number of 50,000, in the sub-channel with LSVF mixing vanes, the size of the local average Nusselt number does not change significantly according to the rod position. Therefore, the heat transfer enhancement in the sub-channel with the LSVF mixing vanes is more valid in a larger Reynolds number flow and the deviation according to the rod position will decrease.

3. Conclusions

In the rod bundle sub-channel spacer grid with Split mixing vanes and LSVF mixing vanes, at Reynolds numbers of 30,000 and 50,000, the changes in the heat transfer enhancement characteristics were compared. In this study, it was found that at a Reynolds number of

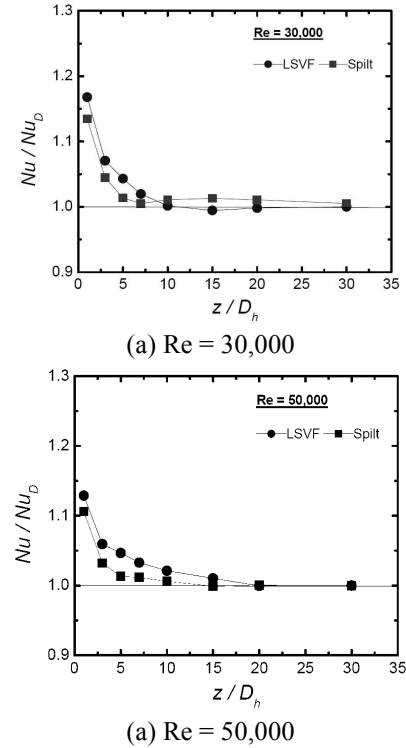


Fig. 7. Axial decay of averaged Nusselt number of rod bundles after the spacer grids with Split and LSVF mixing vanes for Reynolds numbers of 30,000 and 50,000.

30,000, for the LSVF mixing vane between the 1 to 10 D_h section, the average Nusselt number increased 1 to 2 % more than with the Split mixing vane, and then decreased by about 1 percent after 10 D_h . However, at a Reynolds number of 50,000, the average Nusselt number increased 3 % more in the sub-channel with LSVF mixing vanes than with Split mixing vanes between the 1 to 15 D_h section.

4. Acknowledgements

This work was supported by the National Research Foundation of Korea (NRF) grant funded by the Korea government (MSIP). (No. 2012M2A8A2025635)

REFERENCES

- [1] C. M. Lee, J. S. An, Y. D. Choi, Thermo-Hydraulic Characteristics of Hybrid Mixing Vanes in a 17×17 Nuclear Rod Bundle, Journal of Mechanical Science and Technology, Vol. 21, pp. 1263-1270, 2007.
- [2] C. M. Lee, Y. D. Choi, Comparison of Thermo-Hydraulic Performance of Large Scale Vortex Flow (LSVF) and Small Scale Vortex Flow (SSVF) Mixing Vanes in 17×17 Nuclear Rod Bundle, Nuclear Engineering and Design, Vol. 237, pp. 2322-2331, 2007.